frontiers | Frontiers in Physics

TYPE Brief Research Report
PUBLISHED 10 November 2022
DOI 10.3389/fphy.2022.1047445

Check for updates

OPEN ACCESS

EDITED BY
Zhi-Han Zhu,
Harbin University of Science and Technology, China

REVIEWED BY
Zhanda Zhu,
Beijing University of Technology, China
Lijun Qiao,
Taiyuan University of Technology, China

*CORRESPONDENCE
Xinmin Fan,
xinminfan@163.com

SPECIALTY SECTION
This article was submitted to Optics and Photonics,a section of the journal Frontiers in Physics

RECEIVED 18 September 2022
ACCEPTED 31 October 2022
PUBLISHED 10 November 2022

CITATION
Li S, Zhang J, Cheng X, Shao M, Liu Q, An J, Li S and Fan X (2022), Research on beam quality control technology of 2 μm antimonide semiconductor laser. *Front. Phys.* 10:1047445. doi: 10.3389/fphy.2022.1047445

Research on beam quality control technology of 2 μm antimonide semiconductor laser

Sensen Li[1], Jingsheng Zhang[1], Xiangzheng Cheng[2], Ming Shao[2], Qianghu Liu[1], Jiashuo An[3], Shun Li[4,5] and Xinmin Fan[4,5]*

[1]Science and Technology on Electro-Optical Information Security Control Laboratory, Tianjin, China, [2]Key Laboratory of Electro-Optical Countermeasures Test and Evaluation Technology, Luoyang, China, [3]Center for Advanced Laser Technology, Hebei University of Technology, Tianjin, China, [4]School of Physics and Electronic Information, Weifang University, Weifang, China, [5]Weifang Key Laboratory of Laser Technology and Application, Weifang University, Weifang, China

Antimonide semiconductor laser is a new type of laser with unique advantages in the 2 μm band. However, employing FP cavities causes multiple transverse modes to degrade beam quality despite achieving higher power output. In this paper, an antimonide semiconductor laser operating in 2 μm band is realized by utilizing fiber coupling and combining. Fiber combining results in higher output power, while the uniform patterns in both near-field and far-field are obtained, and the beam quality is improved. The experimental results illustrate that the output power reaches 1.2 W after 7-channel beam combination, and the near-field distribution is approximately Gaussian, while the far-field distribution is a flat-top.

KEYWORDS

shortwave infrared laser, antimonide, semiconductor laser, fiber combining, beam quality

Introduction

The laser in 2 μm band is superior to the low atmospheric extinction ratio and human eye safety, and has absorption peaks at various molecules such as H_2O and CO_2 [1, 2]. Therefore, the 2 μm band laser has a vital role in the fields of laser remote sensing, laser ranging, spectroscopy and medical treatment [3–6]. In particular, antimonide semiconductor lasers are gradually occupying an increasingly important position in short-wave infrared lasers due to their small size, high photoelectric conversion efficiency, and good temperature stability [7].

As narrow-bandgap semiconductor materials, antimonide covers the bandwidth of 1.5–5 μm, and thus becomes an ideal material system for mid-infrared semiconductor laser. Antimonide semi-conductor laser is a new type of laser. Since its invention in 1986, the short-wave infrared (2 μm) laser generated by antimonide semiconductor laser has been a research hotspot, and become a high-quality light source for infrared laser countermeasure, biological microscope, medical illumination, laser pumping, plastic welding and other fields [8]. In recent years, antimonide infrared lasers have been widely concerned and developed rapidly. In

2009, Li et al. reported a quantum well antimonide semiconductor laser with a 43 mW CW output at 2.2 μm [9]. In 2010, Niu et al. achieved a 2 μm laser output at room temperature for the first time using an F-P cavity [10]. Subsequently, the wavelength of the output laser was extended to 2.4 μm [11], and the output power was further increased to 1.4 W [12]. In 2011, Reboul et al. reported a GaSb-based semiconductor laser output in the 2 μm band [13]. In 2013, Apiratikul et al. achieved a 40 mW single longitudinal mode laser output in the 2 μm band through laterally coupled distributed feedback [14]. In 2016, Hosoda et al. reported a high-power cascaded antimonide semiconductor laser that achieved a continuous-light laser output with an average power of 2 W at room temperature [15]. In recent years, Niu Zhichuan's team at the Chinese Academy of Sciences has also achieved a series of research results in antimonide semiconductor lasers [12, 16, 17].

Similar to other semiconductor lasers, the 2 μm antimonide semiconductor laser also has problems such as multimode output, large divergence angle, and asymmetric laser pattern, which seriously restrict its development and application. To solve these problems, Rong et al. proposed a fishbone-shaped microstructure in 2016 to reduce the transverse divergence angle of the beam by 55% [18]. In this paper, we employ fiber coupling and combining to improve the beam quality of 2 μm antimonide semiconductor laser. Through 7-channel beam combination, the laser with a center wavelength of 2,055 nm and a line width of 30 nm has an average output power of 1.2 W, while possessing an approximate Gaussian near-field distribution and a flat-topped far-field distribution.

Fiber homogenization theory

A simple and effective beam shaping method is to couple the semiconductor laser into a large-core multimode fiber with a certain length. The outgoing beam is homogenised after transmission due to the limitations of the multimode fibre waveguide structure.

The high-order mode fiber applied to beam shaping is essentially a multimode fiber. The normalized frequency is given by

$$V = \frac{2\pi a NA}{\lambda} \tag{1}$$

where NA is the numerical aperture of the fiber. It can be seen that a larger NA and core diameter results in a more significant normalized frequency of the fiber and a larger number of modes allowed in the fiber, which can be expressed as

$$M \cong \frac{V^2}{2} \tag{2}$$

Due to the larger core diameter and NA of the multimode fiber, i.e., more supported modes, the laser coupling into multimode fiber excites higher-order modes, and most of the energy of the fundamental mode is transferred to the higher-order modes supported by the multimode fiber, and the energy coupling between these modes occurs. Assuming that the intensity of the incident beam is E_{in} $(x, y, z = 0)$, the intensity at the fusion surface after the beam enters the multimode fiber becomes the result of the superposition of each mode:

$$E_{in}(x, y, z = 0) = \sum_1^M \sum_1^N C_{mn} e_{mn}(x, y, z = 0) \tag{3}$$

where $e_{mn}(x, y, z = 0)$ is the intensity distribution of the mn-th order guided mode in the multimode fiber, M × N is the number of excited modes in the multimode fiber, C_{mn} is the modal expansion coefficient and can be expressed as

$$C_{mn} = \frac{\iint_s E_{\mathrm{in}}(x, y, 0) \times e^*_{mn}(x, y, 0) ds}{\iint_s |e_{mn}(x, y, 0)|^2 ds} \tag{4}$$

After these modes propagate for a certain distance in the fiber, the power carried by each conduction mode becomes stable, and the energy is redistributed among the higher-order modes. The final beam intensity distribution from the fiber is the superposition of the various-order modes:

$$E_{out}(x, y, L) = \sum_1^M \sum_1^N C_{mn} e_{mn}(x, y, 0) e^{-i\beta_{mn} L} \tag{5}$$

where mn is the propagation constant of the mn-th order excitation mode of the waveguide in the multimode fiber. The more significant the difference between the diameter of the incident laser pattern and the core diameter of the multimode fiber, the more high-order modes are excited, and the better the homogenization effect of the laser pattern is.

Experimental results and discussion

Direct output performance

In this experiment, the antimonide semiconductor laser chip operating in 2 μm band is designed with a high-reliability ridge waveguide structure and a Fabry-Perot cavity type, using antimonide substrate, grown by quantum well epitaxy, and then packaged in COS. We measured the intensity distribution of the laser direct output, as shown in Figure 1. Figure 1 shows the near-field distribution of the beam at three different positions, 20, 100, and 200 mm from the laser output port, respectively. Obviously, the beam quality is relatively poor, and there are problems such as multimode output, large divergence angle, asymmetric laser pattern, etc. Next, we investigated how to improve the beam quality through multi-beam combination through the fibers.

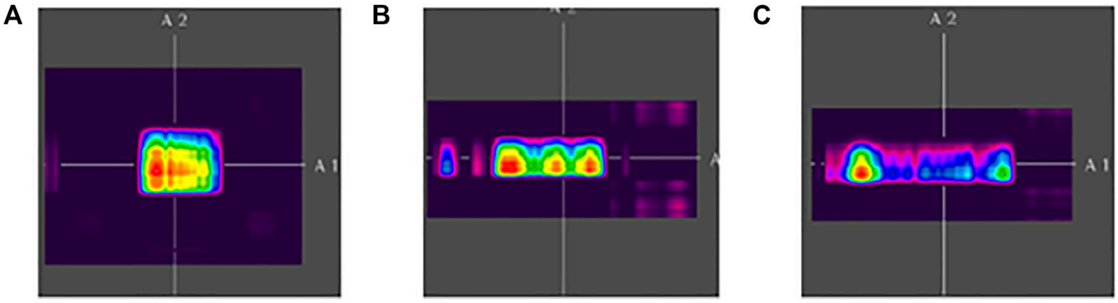

FIGURE 1
The beam near-field distribution at different transmission distances **(A)** 20 mm, **(B)** 100 mm and **(C)** 200 mm.

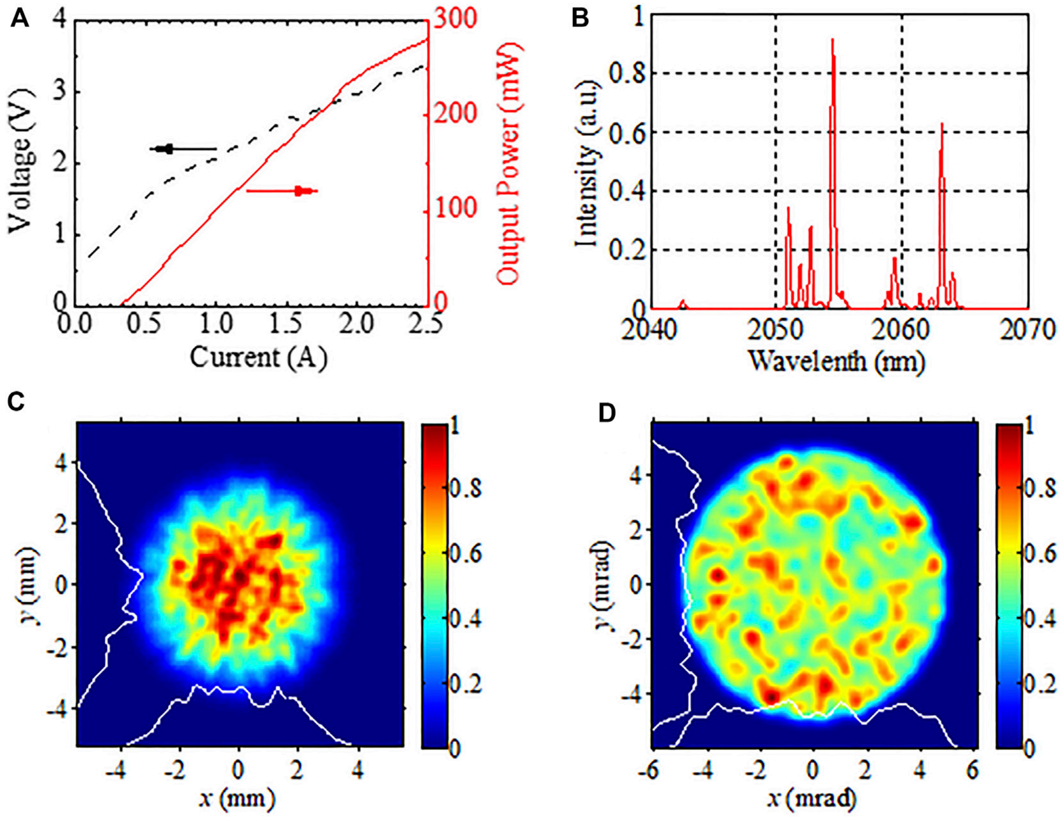

FIGURE 2
Laser output performance of antimonide fiber-coupled semiconductor laser module: **(A)** PIV curve, **(B)** laser spectrum, **(C)**near-field pattern and **(D)**far-field pattern of output beam. The near-field distribution is Gaussian and the far-field distribution is flat-topped.

Single fiber-coupled output performance

The experiments first examined the output of a single laser chip coupled to a quartz fibre with the core diameter of 105 μm. Although the larger the fiber core diameter and numerical aperture, the higher the coupling efficiency, the coupling fiber core diameter must not be too large and must be smaller than the core diameter of the combining fiber. So we choose a core diameter of 105 μm for the coupling fiber. The coupling method adopts a wedge-shaped fiber lens for direct coupling, and the structure of the fiber output port is SMA905.

The variation curve of fiber output power with current is shown in Figure 2A. The overall linearity is relatively good, and the coupling efficiency at the highest power point reaches 56% (when the fiber input power is 0.5 W, the output power is 0.28 W). The end face of the fiber lens is not coated, and the coupling efficiency will be further improved if the coating is applied. The output laser spectrum has a dendritic spectral distribution, about 2,050–2,065 nm, the line width is up to 15 nm, and there are multiple longitudinal modes, as shown in Figure 2B. This is due to the limited frequency selection capability of the FP cavity. If the DFB structure is employed, the narrow linewidth output can be achieved, although the output power will be significantly reduced [19]. Figure 2C shows the near-field distribution of the laser at the output end of the fiber, which is Gaussian as a whole and has modulation inside; Figure 2D shows the far-field distribution of the laser output, which has a flat-top distribution as a whole, and the internal modulation is still evident. It can be seen that the beam quality of the antimonide semiconductor laser in the 2 μm band is still relatively poor after coupling the fiber, because the semiconductor chip itself has multi-transverse mode output and the coupling fiber is a multi-mode fiber. However, compared to Figure 1, it can be seen that the intensity distribution of the beam after transmission through the coupling fiber and tends to be uniformly smooth overall, and the horizontal divergence angle becomes smaller and almost equal to the vertical one, that's because the laser coupling into multimode fiber excites higher-order modes, and most of the energy of the fundamental mode is transferred to the higher-order modes supported by the multimode fiber, and the energy coupling between these modes occurs. From this it can be assumed that if such multi-channel beams are combined into a single multimode fiber, this results in a number of light intensity components with different intensity distributions in different modes being coupled and superimposed, and the beam quality should be further improved, and the greater the number of fiber channels the greater the probability that the intensity of the beam-combining will be uniform. In our experiment, we combine 7-channel optical fiber outputs to explore the feasibility of this method, and verify its effect on the beam quality.

Comparing Figures 1, 2, it can be seen that the intensity distribution of the beam after transmission through the coupling fiber and tends to be uniformly smooth overall, that's because the laser coupling into multimode fiber excites higher-order modes, and most of the energy of the fundamental mode is transferred to the higher-order modes supported by the multimode fiber, and the energy coupling between these modes occurs. But the quality of this beam is still relatively poor and the transverse distribution of the intensity is very uneven. If such multi-channel beams are combined into a single multimode fiber, this results in a number of light intensity components with different intensity distributions in different modes being coupled and superimposed, and the beam quality should be further improved, and the greater the number of fiber channels the greater the probability that the intensity of the beam-combining will be uniform. In our experiment, we combine 7-channel optical fiber outputs to explore the feasibility of this method, and verify its effect on the beam quality.

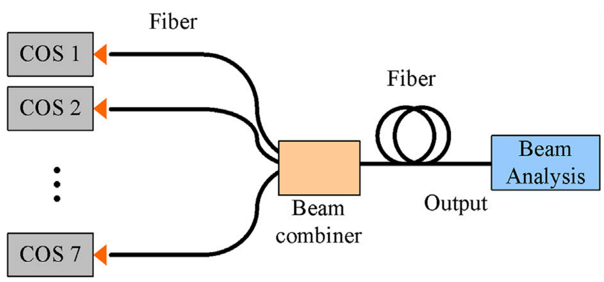

FIGURE 3
The structure of the 7-channel fiber combining.

7-Channel beam combining output performance

Figure 3 is a schematic diagram of the 7-channel fiber combining. Seven identical antimonide semiconductor lasers are respectively coupled and output through the same 105 μm core-diameter fibers, and then combined into another fiber with a core diameter of 200 μm through a beam combiner.

Figures 4A,B shows the output optical power and spectral line characteristics of the 7-channel beam combination. The output laser power of the single-tube COS chip is 0.5 W, the output power of the 7-channel combined beam reaches 1.25 W, and the overall beam combining efficiency of the system is 35.7%. The output laser spectral distribution is from 2,040 to 2,070 nm, showing a dendritic spectral distribution with a line width of up to 30 nm. The near-field and far-field distributions of the output beam are shown in Figures 4C,D, presenting a Gaussian distribution and a flat-top distribution, respectively. Compared with Figures 2C,D, it can be seen that the beam quality is greatly improved after combining, this is consistent with the previous speculation, if increase the number of channels the beam quality and intensity distribution will be further improved.

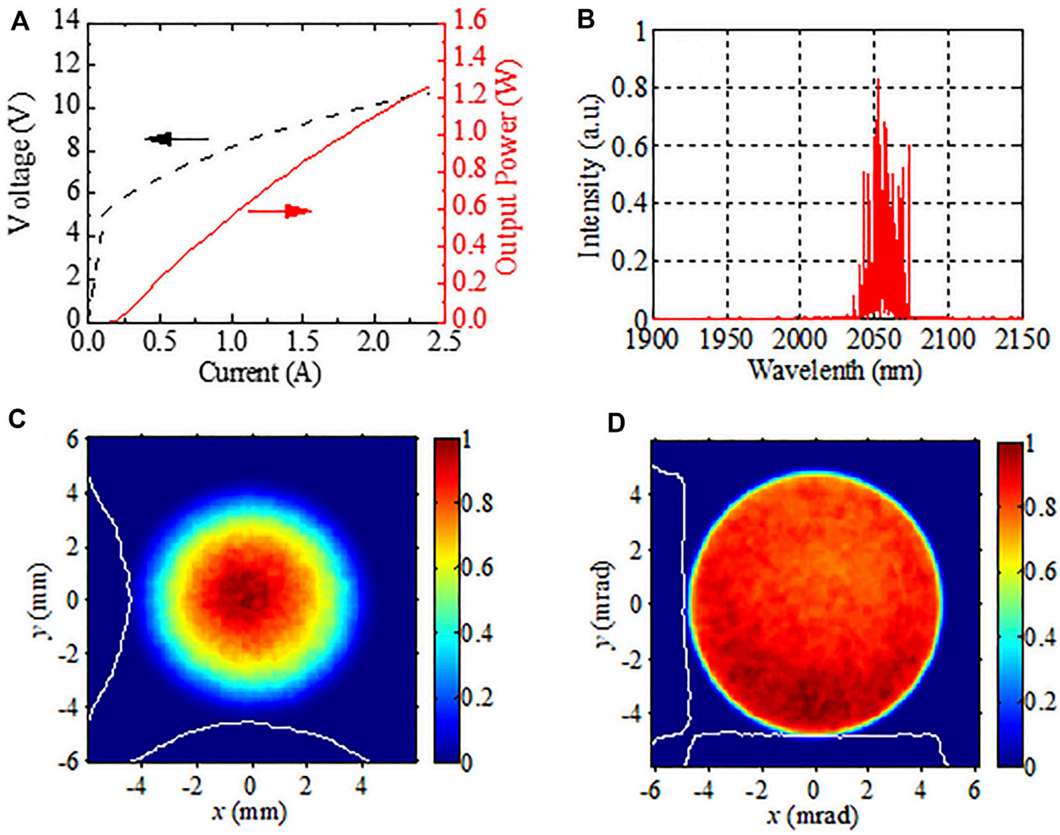

FIGURE 4
Laser output performance of 7-channel beam combining: **(A)** PIV curve, **(B)** laser spectrum, **(C)** near-field pattern and **(D)** far-field pattern.

Conclusion

To address the poor beam quality of antimonide semiconductor lasers in the 2 μm band, we propose a solution to improve the beam quality by using multi-channel fibres to combine beam. In the experiment, the fiber was employed to study the beam combination of 2 μm band antimonide semiconductor lasers coupled with seven channels of fibers. The results indicate that the beam quality is greatly improved after the beam combination, and the near-field distribution is approximately Gaussian, while the far-field exhibits a flat-top distribution. This is due to the poor quality of the output beam of the single-channel fiber, and the lateral distribution of the intensity is very uneven. When the multiplexing is performed, the lowest point of the intensity of a certain beam is likely to be superimposed with the strongest point of the other beams and tend to the average value. Moreover, more beams participating in beam combining will bring more desirable beam quality, that is, the lateral intensity distribution of the beam will be smoothed with an improved the total output power.

Data availability statement

The raw data supporting the conclusion of this article will be made available by the authors, without undue reservation.

Author contributions

SeL: Conceptualization, Drafting the manuscript, and Funding acquisition. JZ: Analysis of data, Data Curation. XC: Investigation. MS: Investigation and Editing. QL: Investigation and Validation. JA: Writing and Acquisition of data. ShL: Acquisition of data and Writing. XF: Conceptualization and Manuscript.

Conflict of interest

The authors declare that the research was conducted in the absence of any commercial or financial relationships that could be construed as a potential conflict of interest.

Publisher's note

References

1. Scholle K, Lamrini S, Koopmann P, Fuhrberg P. 2 μm laser sources and their possible applications. In: B Pal, editor. *Frontiers in guided wave Optics and optoelectronics*. Norderstedt, Germany: Books on Demand (2010). doi:10.5772/39538

2. Pal A, Sen R, Bremer K, Yao S, Lewis E, Sun T, et al. All-fiber" tunable laser in the 2 μm region, designed for CO_2 detection. *Appl Opt* (2012) 51(29):7011–5. doi:10.1364/ao.51.007011

3. Wang Q, Geng J, Jiang S. 2-μm fiber laser sources for sensing. *Opt Eng* (2014) 53(6):061609. doi:10.1117/1.oe.53.6.061609

4. Degnan JJ. Satellite laser ranging: Current status and future prospects. *IEEE Trans Geosci Remote Sens* (1985) 23(4):398–413. doi:10.1109/tgrs.1985.289430

5. Civis S, Horká V, Simecek T, Hulicius E, Pangrac J, Oswald J, et al. GaSb based lasers operating near 2.3 μm for high resolution absorption spectroscopy. *Spectrochimica Acta A: Mol Biomol Spectrosc* (2005) 61(13):3066–9. doi:10.1016/j.saa.2004.11.029

6. Gaimard Q, Nguyen-Ba T, Larrue A, Cerutti L, Rouillard Y, Teissier R, et al. Distributed - feedback GaSb - based laser diodes in the 2.3 to 3.3 μm wavelength range. In: K Panajotov, M Sciamanna, A Valle, R Michalzik, editors. *Semiconductor lasers and laser dynamics vi*. Washington, United States: SPIE (2014). p. 9134.

7. Xie S, Yang C, Huang S, Yuan Y, Zhang Y, Shang J, et al. 2.1 μm InGaSb quantum well lasers exhibiting the maximum conversion efficiency of 27.5% with digitally grown AlGaAsSb barriers and gradient layers. *Superlattices and Microstructures* (2019) 130:339–45. doi:10.1016/j.spmi.2019.05.002

8. Chiu TH, Tsang WT, Ditzenberger JA, van der Ziel JP. Room-temperature operation of InGaAsSb/AlGaSb double heterostructure lasers near 2.2 μm prepared by molecular beam epitaxy. *Appl Phys Lett* (1986) 49(17):1051–2. doi:10.1063/1.97471

9. Li ZG, Liu GJ, You MH, Li L, Li M, Wang Y, et al. 2.0 μm room temperature CW operation of InGaAsSb/AlGaAsSb laser with asymmetric waveguide structure. *Laser Phys* (2009) 19(6):1230–3. doi:10.1134/s1054660x09060085

10. Zhang Y, Tang B, Xu Y, Xu Y, Song G. Molecular beam epitaxy growth of in GaSb/AlGaAsSb strained quantum well diode lasers. *J Semicond* (2011) 32(10):103002. doi:10.1088/1674-4926/32/10/103002

11. Xing JL, Zhang Y, Liao YP, Wang J, Xiang W, Xu YQ, et al. Room-temperature operation of 2.4 μm InGaAsSb/AlGaAsSb quantum-well laser diodes with low-threshold current density. *Chin Phys Lett* (2014) 31(5):054204. doi:10.1088/0256-307x/31/5/054204

12. Xie SW, Zhang Y, Yang CA, Huang SS, Yuan Y, Zhang Y, et al. High performance GaSb based digital-grown InGaSb/AlGaAsSb mid-infrared lasers and bars. *Chin Phys B* (2019) 28(1):014208. doi:10.1088/1674-1056/28/1/014208

13. Reboul JR, Cerutti L, Rodriguez JB, Grech P, Tournie E. Continuous-wave operation above room temperature of GaSb-based laser diodes grown on Si. *Appl Phys Lett* (2011) 99:121113. doi:10.1063/1.3644983

14. Apiratikul P, He L, Richardson CJK. 2 μm laterally coupled distributed-feedback GaSb-based metamorphic laser grown on a GaAs substrate. *Appl Phys Lett* (2013) 99(12):231101. doi:10.1063/1.4808265

15. Hosoda T, Tao F, Leon S, Kipshidze G, Belenky G. High power cascade diode lasers emitting near 2 μm. *Appl Phys Lett* (2016) 108:131109. doi:10.1063/1.4944553

16. Zhang Y, Yang C-A, Shang J-M, Chen YH, Wang TF, Zhang Y, et al. GaSb-based type-I quantum well cascade diode lasers emitting at nearly 2-μm wavelength with digitally grown AlGaAsSb gradient layers*. *Chin Phys B* (2021) 30(9):094204. doi:10.1088/1674-1056/abe930

17. Yang C-A, Zhang Y, Shang J-M, Chen Y, Wang T, Tong H, et al. Research progress of 2-4μm mid-infrared antimonide semiconductor lasers(invited). *Infrared Laser Eng* (2020) 12:163–71. doi:10.3788/IRLA.13_INVITED-1075

18. Rong JM, Xing E, Zhang Y, Wang L, Shu S, Tian S, et al. Low lateral divergence 2 μm InGaSb/AlGaAsSb broad-area quantum well lasers. *Opt Express* (2016) 24(7):7246–52. doi:10.1364/oe.24.007246

19. Zhao Z, Bai Z, Jin D, Qi Y, Ding J, Yan B, et al. Narrow laser-linewidth measurement using short delay self-heterodyne interferometry. *Opt Express* (2022) 30(17):30600–10. doi:10.1364/OE.455028